A Hybrid Swing-Assistive Electro-Hydrostatic Bionic Knee Design

A Hybrid Swing-Assistive Electro-Hydrostatic Bionic Knee Design

Marco Puliti, Federico Tessari, Renato Galluzzi, Simone Traverso, Andrea Tonoli,
Lorenzo De Michieli, and Matteo Laffranchi

***Abstract*— The paper presents a novel, semi-active, bionic knee design for transfemoral amputees. The research exploits a linear electro-hydrostatic actuation (EHA) unit, in series with a flow control hydraulic valve, to assist deambulation tasks. High torque, low speed tasks are managed by the hydraulic valve. Conversely, the EHA is exploited in low torque tasks, either in actuation or regeneration mode. Traditional biomechanical requirements are discussed and revised to propose a human-centered design. Specifically, the focus is towards amputees comfort and prosthesis fluidity over intact limb motion achievement. The mechatronic design is optimized exploiting a multi-objective evolutionary genetic algorithm and validated by means of computational fluid dynamic (CFD) numerical analyses. Additionally, estimates about mass and size are provided. Finally, a knee prosthesis multi-body model is used to numerically validate the proposed design.**

I. Introduction

In the U.S., an estimate of 185 thousand persons undergo an amputation of either upper or lower limb every year [1]. Data from 2005 showed an estimate of 1.6 million U.S. individuals living with the loss of a limb [2]. From those figures, around 42% were major procedures, such as transfemoral amputations (TFAs). The forecast for 2050 is 3.6 million amputees, estimating 1.5 million of major amputations. Accounting for TFAs, patients often walk slower, exhibit a higher frequency of joint injuries and fall risk than able-bodied individuals [3]–[5].

Several types of knee prostheses have been developed to help people with TFAs restore part of the lost limb functionalities [6]. To accomplish such tasks, passive devices were developed at first. In those, stance-knee stability is often achieved through a hyperextension stop. Conversely, the swing phase is facilitated by a passive damper that yields a variable joint impedance, useful to both avoid impact at full knee extension and limit excessive knee flexion during swing. Prostheses featuring such characteristics are often called microprocessor-controlled knees (MPKs), and the Ottobock C-leg is a successful example [7]. Fluidity, ease-of-use and compact size are the main advantages of these devices. However, gait asymmetries, lack of robustness and increased metabolic energy expenditure are the main limitations.

In the last decade, research has focused on powered/active knee prosthesis [8], [9]. Here, the knee joint features a powered transmission system, enabling full support for the wearer. Unlike passive devices, these knee joints are able to move along a predefined trajectory during the swing phase, thus increasing the robustness of the movement. Moreover, active knee prostheses can provide assistance for other tasks, including stairs and ramp ascending/descending and sit-to-stand movements [10]. Although intact limb movements can be achieved, mass, size and noise represent relevant limitations for amputees. In addition, the combination of high joint impedance and artificial movement coordination often leads to discomfort for amputees [11], [12].

To cope with such design issues, recent studies tried to summarize the most relevant prosthesis characteristics for transfemoral amputees [13]. Among all, amputees comfort, prosthesis fluidity and stability are considered more relevant than able-bodied motion achievement. In the attempt to satisfy such requirements, a new line of research has recently emerged, focusing on hybrid semi-active solutions [14], [15]. In these, the prosthesis features a passive damper and an actuator, so that active power can be injected on demand. Such reasoning mainly allows to reduce size and weight of the prosthesis, in favor of amputees comfort and prosthesis compactness. Currently, research on semi-active prosthesis has mainly focused on electro-mechanical actuation [16], [17]. Although their efficiency is remarkable, wear and fatigue are critical aspects for high-duty cycles tasks such as human locomotion. Moreover, their limited backdrivability could impact the prosthesis fluidity. More recently, hydraulic actuation has gained interest in the scientific community [18], [19]. In this context, electro-hydrostatic actuation (EHA) seems to be a promising trade-off between mechanical and hydraulic actuation, since it combines their key benefits. Hydraulically, EHAs benefit from the high power-to-mass ratio; whereas, a quasi-rigid coupling between actuation and load allows to attain large bandwidth dynamics and accurate motion control [20].

Taking into account those factors, the proposed work aims at combining the advantages of passive and active devices, with the aim of yielding a highly backdrivable prosthesis with contained mass and size, able to improve the deambulation of transfemoral amputees. Differently from other semi-active solutions [10], [11], this work aims at demonstrating how a careful and well-thought definition of the biomechanical requirements, combined with a prosthesis actuation topology that well suits backdrivability and integration, can overcome the current limitations of lower limb amputees.

To reach the desired objective, the authors propose a novel

M. Puliti, F. Tessari, S. Traverso, L. De Michieli and M. Laffranchi are with the Rehab Technologies Lab, Italian Institute of Technology, Via Morego 30, 16163, Genova, Italy.

R.Galluzzi is with the School of Engineering and Sciences, Tecnologico de Monterrey, Calle del Puente 222, 14380 Mexico City, Mexico.

M. Puliti and A. Tonoli are with the Laboratory of Mechatronics (LIM), Politecnico di Torino, Corso Duca degli Abruzzi 24, 10129, Turin, Italy.

prosthesis layout that consists of a motor-driven hydraulic valve (i.e., MPK hydraulic damper), to mainly deal with torque demanding tasks, and a linear electro-hydrostatic actuator (EHA) to address high speed tasks. The prosthesis will retain the desirable characteristics of a passive device, with the possibility to inject active power when needed. Once presented the rationale behind the biomechanical parameters selection, and the subsequent design of a custom and integrated EHA knee prosthesis, the work will focus on validating the performances achieved by means of CFD and multibody simulations.

II. Biomechanical Requirements

Considering the work from Grimmer *et al.* [21] as biomechanical reference for healthy subjects, the design objectives can be summarized in **(i)** user mass, **(ii)** prosthesis achievable tasks, **(iii)** range of motion (ROM), **(iv)** desired knee torque-speed characteristic, and **(v)** prosthesis mass. The 50^{th} american men percentile was considered as target user mass, corresponding to 78.4 kg (i.e., 63^{th} percentile in women) [22].

The next target concerns the EHA role in the proposed prosthesis design. As previously stated, knee actuation can be beneficial in different deambulation stages. Table I lists the main bipedal activities, along with their daily occurrence and metabolic cost. Level walking has the highest occurrence per day; therefore representing the main design focus. Although stairs ascending and sit-to-stands represent relevant actuation tasks, their occurrence is considerably lower than level walking. Moreover, such tasks are characterized by high torque requirements, up to 100 Nm [23], rendering a heavy and bulky actuator. Nonetheless, these tasks would be handled by the EHA, providing a percentage of the biomechanical requirement for healthy subjects. On the other hand, it seems worth designing the electro-hydrostatic actuation for the swing phase of walking since the required torque content is considerably lower than in stance. Moreover, high speed braking tasks such as part of the swinging can be efficiently exploited to regenerate part of the energy through the EHA.

On the other hand, the hydraulic valve can handle the stance phase, in which the high damping request and the relatively low speeds achieved do not favor the usage of the EHA in regeneration mode. Additionally, the hydraulic damper can be also exploited for stairs and ramp descending, as passive devices have shown to be quite effective to cope with high torque tasks [31]–[33]. Finally, active and passive sides could also work simultaneously to maximise the EHA energy convertion.

TABLE I: Gait cycle activities [24]–[30]

Task	**Occurrence/day**	**Metabolic cost V_{O2} [ml/(kg·min)]**
Walking	1500 steps (TFA) 5500 steps (healthy)	14.2 (TFA) 9 (healthy)
Stairs ascending	47-66 stairs (healthy)	33.5 (healthy)
Stairs descending	47-66 stairs (healthy)	17 (healthy)
Sit-to-Stand (StS)	33-71 StS (healthy)	3.8 (healthy)

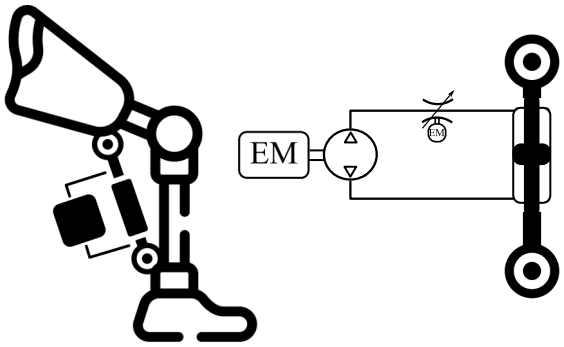

Fig. 1: Hybrid prosthetic knee schematic. Overall prosthesis architecture (left). Details of the hybrid actuation scheme. The motor-pump unit represents the EHA, whereas the flow control valve is represented as a motorized variable resistance (right).

The prosthesis schematic is presented in Figure 1. The series connection among motor-pump unit (i.e., active) and flow-control valve (i.e., passive) sides allows for minimizing the number of hydraulic components. In addition, a through rod cylinder avoids using an hydraulic accumulator.

The next biomechanical target is the knee range of motion. Taking healthy subjects as reference [27], a 110 degrees ROM is expected in deambulation, 100 for knee flexion and 10 for the extension. Concerning the knee torque-speed desired behaviour, Figure 2 presents the walking gait trajectory, qualitatively highlighting passive and active tasks. The speed requirement is -65 rpm (6.8 rad/s) during flexion and 84 rpm (8.8 rad/s) during extension. Such values would theoretically allow amputees to walk up to 6 km/h, corresponding to fast walking [34], [35]. Conversely, the maximum actuation torque requirement is defined by the inertial load during

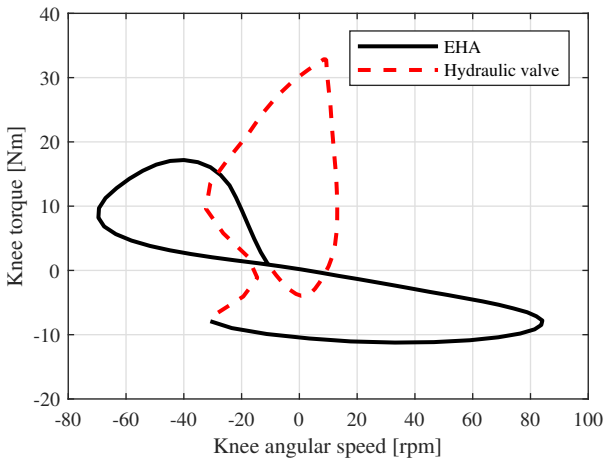

Fig. 2: Knee biomechanical torque-speed profile during level walking for a user of 78.4 kg. In dashed red line the stance phase, while in solid black line the swing phase.

swing, representable as

$$T_{max} = J_{leg} a_{kmax}, \quad (1)$$

in which J_{leg} represents the prosthesis and passive foot inertia and a_{kmax} its maximum angular acceleration. The inertia contribution can be written as

$$J_{leg} = m_{target}(k_{cog}\ L_{k-f})^2, \quad (2)$$

in which m_{target} is the target mass, k_{cog} represents the normalized position of the prosthesis center of gravity with respect to the knee joint and L_{k-f} is the average human leg length from knee to foot joints centers. The prosthesis mass target is set to 2 kg (including battery pack), slightly higher than current passive knee prosthesis [36], [37]; whereas, an average mass of 1.2 kg was considered for both a passive foot and its shoe [38]. According to Winter's biomechanical data [39], L_{k-f} is $0.285H$, in which H is taken as the 50th percentile male human height, 1.76 m. Furthermore, the assumption is that the prosthesis center of gravity is at 45% of the leg length, in line with sound limbs anthropometrical data available in literature [22]. Finally, the maximum acceleration during the walking gait is set to 122.17 rad/s^2, corresponding to fast walking [35]. Overall, the maximum inertial torque during swing is

$$T_{max} = m_{target}\ (0.45 L_{k-f})^2\ a_{kmax} = 19.8\ Nm, \quad (3)$$

As previously stated, the actuation target is to fully provide torque during swing. Nonetheless, such performance can also be exploited to provide assistance up to 61% during level walking stance, 22% during stair ascending and 19% in sit-to-stands, relatively to healthy subjects torque requirements [23]. Such assumption is reinforced by recent studies, in which it emerged that a partial assistance during those tasks can represent a substantial benefit for transfemoral amputees [40]. Overall, the biomechanical requirements are summarized in Table II.

TABLE II: Biomechanical requirements

Description	Symbol	Value	Unit
Maximum swing torque	T_{max}	20	Nm
Maximum stance torque	T_{res}	35	Nm
Maximum knee speed	ω_{max}	84	rpm
Knee range of motion	$\Delta\theta_{rom}$	110	deg
Prosthesis mass target	m_{target}	2	kg
Maximum active power	P_{act}	65	W

III. Mechatronic Design

The mechatronic design mainly concerns the actuation of the knee prosthesis. The choice to use a linear actuator allows for higher hydraulic pressures than the rotary counterpart, due to better sealing capabilities. The EHA features a permanent magnet synchronous machine (PMSM), rigidly connected to a hydraulic gerotor. The design is performed exploiting an evolutionary genetic algorithm (GA). The inputs are maximum torque, angular speed and power, whereas

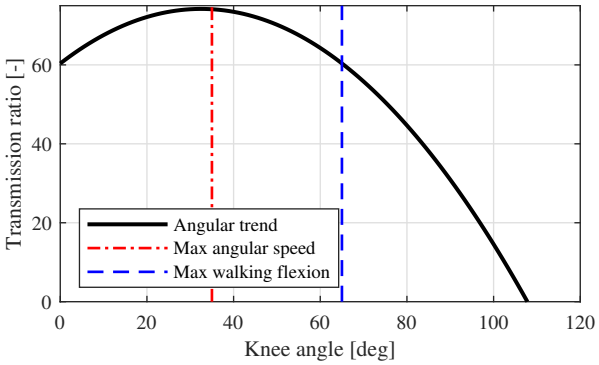

Fig. 3: Overall prosthesis transmission ratio between knee joint rotation and electric motor rotation.

the outputs, also representing the GA fitness functions, are the EHA size and an estimate of the overall efficiency. Constraints on maximum angular speed and transmission efficiency take into account backdrivability properties and noise production. The gerotor has been modeled considering previous analyses conducted [41]; whereas an orifice plate analogy is used to analytically model viscous and friction losses [42].

From a kinematic point of view, the prosthesis is connected to thigh by means of a ball joint; whereas it is integral with respect to the shank. As it is possible to notice from Figure 1 on the left, the hydraulic cylinder creates a variable lever with the knee rotation center, proportional to the knee angle. In addition, the transmission ratio between cylinder cross-section area and gerotor volumetric displacement allows to convert rotary into linear motion. The combination of these kinematic aspects defines the overall transmission ratio, presented in Figure 3 as function of the knee ROM. Its maximum value, $75:1$, corresponds to a knee flexion of 36 degrees. The hydraulic cylinder stroke is 57.5 mm and an estimate of the EHA volume is 60 cc. The electric machine is a TQ RoboDrive ILM38x06, 110 W servo motor. The maximum angular speed is 10500 rpm (1100 rad/s) and its peak torque is 0.302 Nm. Since its duty cycle would be relatively short, it could be operated up to 0.9 Nm, for a short time period. Its maximum efficiency is 88%, with a mass of 53 g.

Conversely, the gerotor machine is a positive displacement hydraulic component, featuring a $6-7$ teeth configuration corresponding to inner and outer gears, respectively. Such device is compact and characterized by low wear and noise if compared to external gear units. Its volumetric displacement is 1.25 cc/rev, with a maximum pressure differential of 25 bar (2.5 MPa) in nominal conditions. The outer diameter is 26 mm, with an axial length of 13 mm. The actuator solid model is presented in Figure 4. By placing the manifold (2 in Figure 4) as close as possible to the pyramidal joint, the prosthesis center of gravity is close to the knee joint, thus diminishing the inertial load. Overall, the mass break-down for the knee prosthesis is summarized in Table III. The estimated total mass is 1.7 kg, 15% below the biomechanical assumption.

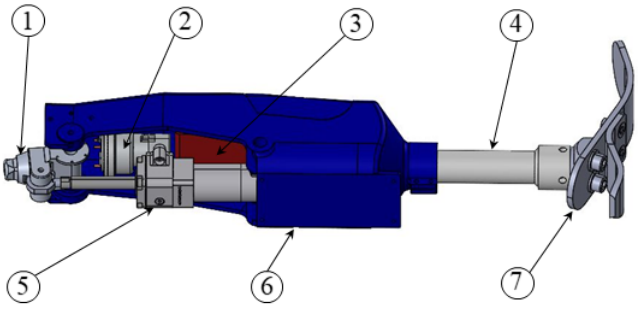

Fig. 4: Hybrid knee prosthesis. 1) Pyramidal knee joint; 2) EHA and valve manifold; 3) Battery; 4) Shank; 5) Hydraulic cylinder; 6) Prosthesis chassis; 7) Passive foot.

Such forecast would further decrease the required torque during swing, while improving the fluidity of the device. To summarize, Table IV presents the prosthesis performance estimate.

IV. Results

The presented semi-active knee prosthesis design is validated through CFD simulations and considering a leg multibody model. Simulations are performed in two operating conditions. In actuation, the electric machine is imposing torque and angular speed (i.e., motor operations), whereas the gerotor behaves as hydraulic pump, resisting such load. On the other hand, when either braking or regenerating, the gerotor acts as hydraulic motor and the electric machine is resisting the load (i.e., generator operations). To account for both conditions, the I and II quadrants of the torque-speed plane where considered. Simulations have been performed within the Simerics PumpLinx environment, considering torques from 0 to 25 Nm, equally spaced, and a -85 to 85 rpm (-8.9 to 8.9 rad/s) interval for the knee angular speed. A fluid density ρ of 840 $\mathrm{kg/m^3}$ and a dynamic viscosity μ_f of 9.4 $\mathrm{kPa/s}$ characterize the fluid considered. In each simulation, the 3D fluid model is simulated for an angular motion transient equal to 4 hydraulic chambers between gears, to avoid effects related to initial conditions. To account for viscous and friction losses, the gerotor radial clearance was set to 10 μm, whereas the axial one to 15 μm, both uniformly distributed. Results are depicted in Figure 5, presenting the extrapolated efficiency maps. For each simulated point, the efficiency is calculated as

$$\eta_{gm} = \frac{T_g\ \omega_g}{\Delta p\ Q_g}, \quad \eta_{gp} = \frac{\Delta p\ Q_g}{T_g \omega_g} \tag{4}$$

for both motoring η_{gm} and pumping η_{gp} operations. As it is possible to notice, the maximum efficiency is around 75% in both operating conditions and not all the simulated points are efficient due to mechanical and viscous losses. Overall, the gerotor machine is performing adequately in the required torque-speed specifications, with compact size and contained mass.

To validate the knee prosthesis design, a leg multibody model has been developed exploiting the MATLAB Simscape environment. The electric machine is piloted with a torque command and modeled through a power loss map in the four quadrants of the torque speed plane. Likewise, the gerotor is modeled by means of 2D efficiency look-up tables. On the other hand, the hydraulic valve behaviour is represented through an efficiency look-up table as function of pressure differential and volumetric flow rate. The simulation considers a stride time of 1.5 s, corresponding to a walking speed of 3.4 km/h (assuming a stride length of 1.42 m, obtained considering a 1.78 m subject - 50th percentile man [23]). Figure 6 presents a schematic of the control strategy implemented. The direct loop features a PID controller,

TABLE III: Estimate prosthesis mass brake-down

Component	Mass [g]
Hydraulic cylinder	400
Electro-hydrostatic actuation	200
Prosthesis cover	600
Battery pack	350
Screw, bolts and misc.	100
Hydraulic valve	50
Total mass	1700

TABLE IV: Hybrid knee performance estimates

Feature	Value
Max. active torque	19.8 Nm
Max. knee speed	84 rpm
Max. active power	70 W
Min./Avg./Max. transmission ratio	10/40/75

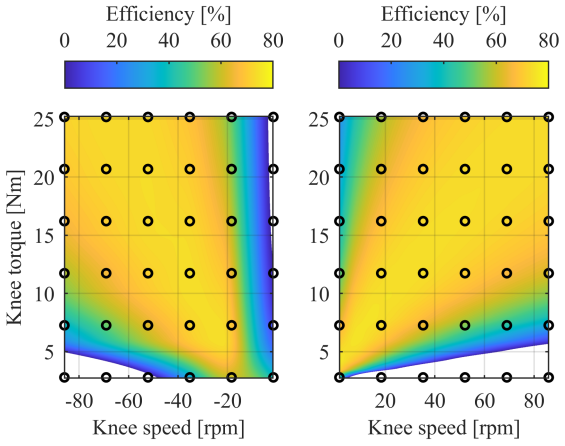

Fig. 5: Hydraulic gerotor unit CFD simulation results. On the right side, the overall efficiency when working as hydraulic pump. On the left side, the overall efficiency when operating as hydraulic motor.

taking the error between reference, considering healthy subject data [23], and extrapolated, simulated through the multibody model, angles as input. Its output is a torque reference to command the electro-hydrostatic actuation. The PID has been tuned by first linearizing the model and then accounting for closed loop stability and adequate robustness and performance.

Finally, a state machine is used to differentiate swing and stance. Namely, in stance, the controller is disabled, the EHA is idling and the angle reference is set to zero. The hydraulic valve opening, θ_v, is triggered to be in fully closed position, to resist the stance load. The latter is taken from healthy subjects biomechanical data and represents the torque transmitted from the leg to the knee joint. Figure 7 presents the error between reference (i.e. 0 degrees) and simulated angles. A positive error represents a knee flexion. Its average value, 2.79 degrees, is mainly related to the valve leakage flow rate, 0.2 l/min. Nonetheless, such behavior can be considered beneficial to initiate the subsequent swing phase [34]. The peak knee torque during stance is around 40 Nm, resorting in a maximum pressure differential of 50 bar (5 MPa) at the valve ends.

Conversely, the EHA torque command is enabled during swing and the hydraulic valve is switched to a fully open position. In this state, the EHA is working both in actuation and breaking/regeneration modes to accommodate the torque-speed requirements of Figure 2. The comparison between reference and simulated angle is highlighted in Figure 8. There is an adequate tracking of the reference knee trajectory, with an average tracking error of 1.49 degrees.

Finally, it is worth investigating the power consumption during the gait cycle. Figure 9 presents the EHA power consumption over the swing cycle, highlighting its root mean square (RMS) and mean values. The RMS is 17.75 W, whereas the average is 14.6 W. Its peak value is 48 W, corresponding to the condition of maximum knee acceleration. The peak current consumption corresponds to 2 A, when the system is supplied by a 24 V battery pack. As it is possible to notice, the last part of the swing is characterized by negative power consumption. Precisely, such interval represents the end of the leg extension in which the knee requires braking to approach heel strike. From an EHA point of view, negative power could represents energy regeneration since the gerotor machine behaves as hydraulic motor and the electric machine as generator. Since the efficiency of the actuation cannot be unitary, only part of such mechanical power can be effectively transformed in electric power.

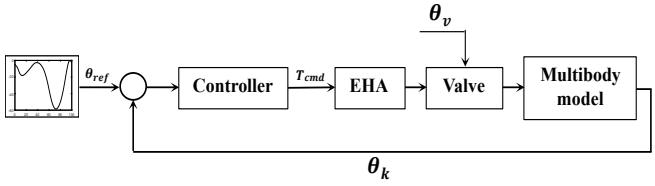

Fig. 6: Prosthesis preliminary control strategy.

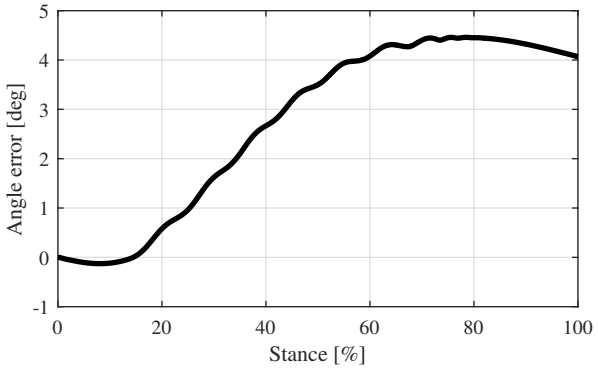

Fig. 7: Knee angle variation during stance phase.

Additionally, the power consumption related to the hydraulic valve motor should be accounted. Considering an off-the-shelf gear motor compliant with the hydraulic valve requirements (i.e., Maxon DCX10S model), an estimate of the peak power consumption is 1 W/stride. Overall, the theoretical average power consumption during one walking gait is around 10 W/stride. Such power corresponds to an energy expenditure of 14 J/stride. Since the knee prosthesis would be supplied by a 24 V battery pack, the energy consumption in terms of current is 0.16 mAh/stride. Considering a commercial LiPo battery with a capacity of 1500 mAh, the knee prosthesis could perform around 9000 strides per battery charging cycle, corresponding to almost 2 days of usage considering healthy subjects data [23]. Such computation represents a best case scenario since the power consumption related to the prosthesis embedded electronics has not been considered. Moreover, such computation does not account for other deambulation tasks, such as stairs ascending/descending and sit-to-stands that could impact the overall prosthesis energy consumption.

V. Discussion

The baseline for the knee prosthesis design concerned a revision of the biomechanical requirements of healthy subjects, favoring amputees comfort and prosthesis fluidity over mechatronic performance. Level walking was considered the

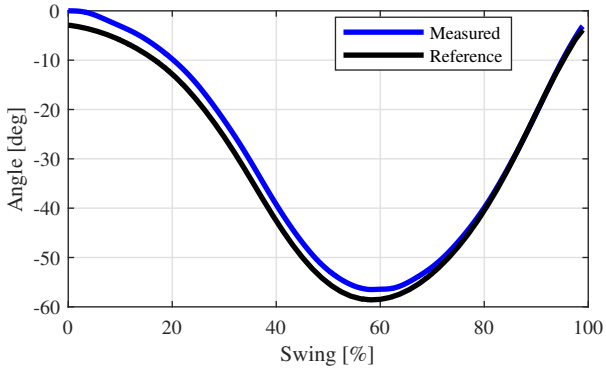

Fig. 8: Knee angle comparison during swing. Reference angle (black curve), measured angle (blue curve).

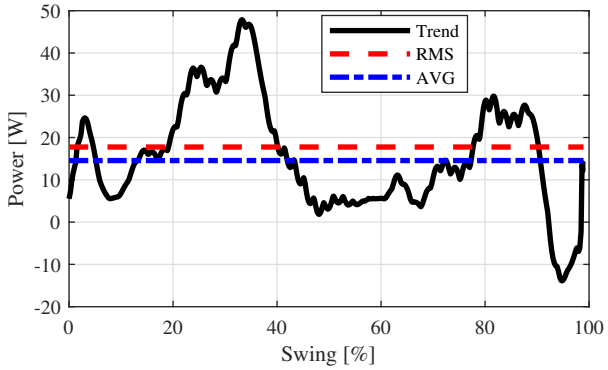

Fig. 9: Power consumption of actuating unit at the power supply, i.e. battery. Trend over time (black curve); RMS value (red, dotted line); mean value (blue, dotted line).

focus of the design since its occurrence per day is the highest when compared with other deambulation tasks. The aim was to enhance the swing phase by providing active power through an electro-hydrostatic actuation unit. On the other hand, a microprocessor controlled hydraulic damper is exploited to attain stance tasks, in which high torque content is required. The EHA design was numerically validated with a CFD analysis of the gerotor hydraulic machine. Results were presented in both motoring and pumping operations, showing a satisfactory performance of the hydraulic unit with a maximum efficiency of 75%. The optimized design yielded a compact, yet performant device in the required torque-speed working region.

Then, to validate the overall knee prosthesis, a leg multibody model was developed. A state machine was implemented to differentiate the two main walking tasks: stance and swing. In the former, the EHA is idling; whereas, the hydraulic valve is fully closed in order to resist the artificial leg load. Results showed a maximum knee flexion of 4.5 degrees and a maximum braking torque of 40 Nm. Conversely, during swing, the hydraulic valve is fully opened, the EHA is commanded with a torque reference and a desired trajectory is imposed to the knee joint. The simulation showed a contained tracking error (RMSE $= 1.48$ degrees) between desired and simulated knee angle, with an average energy consumption of 14 J/stride. Although such value is contained, the power electronics energy consumption has not been considered in the computation. Finally, the estimates in terms of mass, 1.7 kg and size, 60 cc, are contained and comparable with state of the art passive prosthesis devices [7].

VI. Conclusion

The aim of the presented paper was to design a bionic, semi-active knee prosthesis for swing assistance. The device is composed by an hydraulic damper featuring a flow control valve, serially connected to an electro-hydrostatic actuation unit. Such combination allows to benefit from the passive architecture during high torque braking tasks and inject active power on demand. First, a CFD validation of the mechatronic design was presented. Then, a multibody model of the developed bionic limb was implemented to validate the proposed design over a walking gait cycle.

Results showed the prosthesis ability to recreate intact limb movements with contained energy consumption per stride. Such achievement seems promising, yielding a knee prosthesis with a mass comparable to commercial microprocessor knees. The proposed design had the objective to find a trade-off between intact limb motion achievement and amputees comfort, intended as reduced prosthesis weight and size. Concurrently, the possibility to inject active power on demand strongly increase the robustness of the prosthesis. Possible limitations are related to unmodelled parameters and external disturbances that were not included in the multibody simulations. Those could be accounted considering an overall safety factor in the prosthesis design. Additionally, the control strategy objective was to perform a numerical validation. Therefore, more sophisticated and effective strategies could be investigated. Finally, future works will focus on the experimental validation of the proposed semi-active prosthesis architecture.

References

[1] Owings M, Kozak L. Ambulatory and inpatient procedures in the United States, 1996, Vital Health Statistics, 1998, 139, https://pubmed.ncbi.nlm.nih.gov/9866429/

[2] Ziegler-Graham K., MacKenzie E.J., Ephraim P.L. et al., Estimating the prevalence of limb loss in the United States: 2005 to 2050, Archives of Physical Medicine and Rehabilitation, 2008, 89(3), https://doi.org/10.1016/j.apmr.2007.11.005

[3] Gauthier-Gagnon C.,Grise M. C., and Potvin D., Enabling factors related to prosthetic use by people with transtibial and transfemoral amputation, Archives of Physical Medicine and Rehabilitation, 1999, 80(6), pp. 706-13, https://doi.org/10.1016/S0003-9993(99)90177-6

[4] Talbot L. A., Musiol, R. J., Witham E. K., and Metter E. J., Falls in young, middle-aged and older community dwelling adults: perceived cause, environmental factors and injury, BMC Public Health, 2005, 5(86), https://doi.org/10.1186/1471-2458-5-86

[5] Schmalz T., Blumentritt S. and Marx B, Biomechanical analysis of stair ambulation in lower limb amputees, Gait & Posture, 2007, 25(2), pp. 267–278, https://doi.org/10.1016/j.gaitpost.2006.04.008

[6] M. Asif, M.I. Tiwana, U.S. Khan et al., Advancements, Trends and Future Prospects of Lower Limb Prosthesis, IEEE Access, 2021, 9, https://doi.org/10.1109/ACCESS.2021.3086807

[7] Ottobock, https://www.ottobockus.com/prosthetics/lower-limb-prosthetics/solution-overview/c-leg-above-knee-system/

[8] Tran M., Gabert L., Cempini M. and Lenzi T., A Lightweight, Efficient Fully Powered Knee Prosthesis With Actively Variable Transmission, IEEE Robotics and Automation Letters, 2019, 4(2), pp. 1186-1193, https://doi.org/10.1109/LRA.2019.2892204

[9] Lawson B. E., Mitchell J., Truex D., et al., A Robotic Leg Prosthesis: Design, Control, and Implementation, IEEE Robotics and Automation Magazine, 2014, 21(4), pp. 70-81, https://doi.org/10.1109/MRA.2014.2360303

[10] Ledoux E. D. and Goldfarb M., Control and Evaluation of a Powered Transfemoral Prosthesis for Stair Ascent, IEEE Transactions on Neural Systems and Rehabilitation Engineering, 2017, 25(7), pp. 917-924, https://doi.org/10.1109/TNSRE.2017.2656467

[11] Hafner B.J. and Askew R.L., Physical performance and self-report outcomes associated with use of passive, adaptive, and active prosthetic knees in persons with unilateral, transfemoral amputation: Randomized crossover trial, Journal of Rehabilitation Research and Development, 2015, 52(6), pp. 677-700, https://doi.org/10.1682/JRRD.2014.09.0210.

[12] Wolf, E.J., Everding, V.Q., Linberg, A.L., et al., Assessment of transfemoral amputees using C-leg and Power Knee for ascending and descending inclines and steps, Journal of Rehabilitation Research and Development, 2012, 49(6), pp. 831–842, https://doi.org/10.1682/JRRD.2010.12.0234

[13] Fanciullacci, C., McKinney, Z., Monaco V., et al., Survey of transfemoral amputee experience and priorities for the user-centered design of powered robotic transfemoral prostheses, Journal of NeuroEngineering Rehabilitation, 2021, 18(168), https://doi.org/10.1186/s12984-021-00944-x

[14] Lenzi T., Sensinger J., Lipsey J. et al., Design and preliminary testing of the RIC hybrid knee prosthesis, 37th Annual International Conference of the IEEE Engineering in Medicine and Biology Society (EMBC), 2015, pp. 1683-1686, https://doi.org/10.1109/EMBC.2015.7318700.

[15] Lenzi T., Cempini M., Hargrove L. et al., Design, development, and testing of a lightweight hybrid robotic knee prosthesis, The International Journal of Robotics Research, 2018,37(8), pp. 953-976, https://doi.org/10.1177/0278364918785993

[16] Lee J. T., Bartlett H. L. and Goldfarb M., Design of a Semipowered Stance-Control Swing-Assist Transfemoral Prosthesis, IEEE/ASME Transactions on Mechatronics, 2020, 25(1), pp. 175-184, https://doi.org/10.1109/TMECH.2019.2952084

[17] Baimyshev A., Lawson B. and Goldfarb M., Design and Preliminary Assessment of Lightweight Swing-Assist Knee Prosthesis, 40th Annual International Conference of the IEEE Engineering in Medicine and Biology Society (EMBC), 2018, pp. 3198-3201, https://doi.org/10.1109/EMBC.2018.8513087

[18] Tessari F., Galluzzi R., Tonoli A., et al., An Integrated, Back-Drivable Electro-Hydrostatic Actuator for a Knee Prosthesis, 8th IEEE RAS/EMBS International Conference for Biomedical Robotics and Biomechatronics (BioRob), 2020, pp. 708-714, https://doi.org/10.1109/BioRob49111.2020.9224278

[19] Tessari F., Galluzzi R., Tonoli A. et. al, Analysis, Development and Evaluation of Electro-Hydrostatic Technology for Lower Limb Prostheses Applications, International Conference on Intelligent Robots and Systems (IROS), 2020, https://doi.org/10.1109/IROS45743.2020.9341512.

[20] Belloli D., Previdi F., Savaresi S.M. et al., Modeling and Identification of an Electro-Hydrostatic Actuator, IFAC Proceedings Volumes, 2010, 43 (18), pp. 620-625, https://doi.org/10.3182/20100913-3-US-2015.00020.

[21] Grimmer M., Elshamanhory A.A. and Beckerle P., Human Lower Limb Joint Biomechanics in Daily Life Activities: A Literature Based Requirement Analysis for Anthropomorphic Robot Design, Frontiers in Robotics and AI, 2020 (7), https://doi.org/10.3389/frobt.2020.00013

[22] Tilley A.R. and Dreyfuss H. Associates, The Measure of Man and Woman: Human Factors in Design, Revised Edition, 2001

[23] Lencioni, T., Carpinella, I., Rabuffetti, M. et al., Human kinematic, kinetic and EMG data during different walking and stair ascending and descending tasks, Scientific Data, 2019 6(309), https://doi.org/10.1038/s41597-019-0323-z

[24] Halsne E.G., Waddingham M.G. and Hafner B.J., Long-term activity in and among persons with transfemoral amputation, Journal of Rehabilitation Research and Development, 2013 50(4), https://doi.org/10.1682/jrrd.2012.04.0066

[25] Schmalz T., Blumentritt S. and Jarasch R., Energy expenditure and biomechanical characteristics of lower limb amputee gait: the influence of prosthetic alignment and different prosthetic components, Gait & Posture, 2002 16(3), https://doi.org/10.1016/s0966-6362(02)00008-5

[26] Teh K.C. and Aziz A.R., Heart rate, oxygen uptake, and energy cost of ascending and descending the stairs, Medicine & Science in Sports & Exercise, 2002 34(4), https://doi.org/10.1097/00005768-200204000-00021

[27] Grimmer M. and Seyfarth A., Mimicking Human-Like Leg Function in Prosthetic Limbs, Neuro-Robotics: Trends in Augmentation of Human Performance, 2014 2, https://doi.org/10.1007/978-94-017-8932-5-5

[28] Bohannon R.W., Daily sit-to-stands performed by adults: a systematic review, Journal of Physical Therapy Science, 2015 27(3), https://doi.org/10.1589/jpts.27.939

[29] Bhardwaj S., Khan A.A. and Muzammil M., Knee torque estimation in sit to stand transfer, Journal of Physics: Conference series, 2019 1240(012153), https://doi.org/10.1088/1742-6596/1240/1/012153

[30] Júdice P.B., Hamilton M.T., Sardinha L.B. et al., What is the metabolic and energy cost of sitting, standing and sit/stand transitions?, European Journal of Applied Physiology, 2016 (2), https://doi.org/10.1007/s00421-015-3279-5

[31] Kaufman K.R., Levine J.A., Brey R.H. et al., Gait and balance of transfemoral amputees using passive mechanical and microprocessor-controlled prosthetic knees, Gait & Posture, 2007 26(4), pp. 489-493, https://doi.org/10.1016/j.gaitpost.2007.07.011

[32] Lythgo N., Marmaras B. and Connor H., Physical Function, Gait, and Dynamic Balance of Transfemoral Amputees Using Two Mechanical Passive Prosthetic Knee Devices, Archives of Physical Medicine and Rehabilitation, 2010 91(10), pp. 1565-1570, https://doi.org/10.1016/j.apmr.2010.07.014

[33] Johansson J., Sherrill D., Riley P. et al., A Clinical Comparison of Variable-Damping and Mechanically Passive Prosthetic Knee Devices, Journal of Physical Medicine and Rehabilitation, 2005 84(5), pp. 563-575, https://doi.org/10.1097/01.phm.0000174665.74933.0b

[34] Boonstra A.M., Fidler V. and Eisma W.H., Walking speed of normal subjects and amputees: aspects of validity of gait analysis, Prosthetics and Orthotics International, 1993, 2, pp.78-82, https://doi.org/10.3109/03093649309164360

[35] Dauriac B., Bonnet, X., Pillet, H. et al., Estimation of the walking speed of individuals with transfemoral amputation from a single prosthetic shank-mounted IMU, Proceedings of the Institution of Mechanical Engineers, Part H: Journal of Engineering in Medicine, 2019, 233(9), pp. 931–937, https://doi.org/10.1177/0954411919858468

[36] Genium X3 knee, Ottobock Inc., https://www.ottobockus.com/prosthetics/lower-limb-prosthetics/solution-overview/genium-above-knee-system/

[37] Rheo Knee, Ossur Inc., https://www.ossur.com/en-us/prosthetics/knees/rheo-knee

[38] Terion K2 Prosthetic foot, Ottobock Inc., https://www.ottobockus.com/products/1c11-terion.html

[39] Winter David A., Biomechanics and Motor Control of Human Movement, 4th Edition, 2009, https://doi.org/10.1002/9780470549148

[40] Bulea T.C., Kobetic R., Audu M.L. and Triolo R.J., Stance controlled knee flexion improves stimulation driven walking after spinal cord injury, Journal of NeuroEngineering and Rehabilitation, 2013, 10(68), https://doi.org/10.1186/1743-0003-10-68.

[41] Puliti M., Tessari F., Galluzzi R. et al., Design Methodology of Gerotor Hydraulic Machines for Mechatronic Applications, Proceedings of the ASME 2021 International Mechanical Engineering Congress and Exposition, 2021, https://doi.org/10.1115/IMECE2021-73205

[42] Harrison J., Aihara R. and Eisele F., Modeling Gerotor Oil Pumps in 1D to Predict Performance with Known Operating Clearances, SAE International Journal of Engines, 2016 (9), pp.1839-1846, https://doi.org/10.4271/2016-01-1081